plea
ions will be in blue
white

REPORT DOCUMEN

AD-A256 683

Form approved
OMB No. 0704-0188

(2)

Public reporting burden for this collection of information is estimated to average 1 hour per response, including the time for reviewing instructions, searching existing data sources, gathering and maintaining the data needed, and completing and reviewing the collection of information. Send comments regarding this burden estimate or any other aspect of this collection of information, including suggestions for reducing this burden, to Washington Headquarters Services, Directorate for information Operations and Reports, 1215 Jefferson Davis Highway, Suite 1204, Arlington, VA 22202-4302, and to the Office of Management and Budget, Paperwork Reduction Project (0704-0188), Washington, DC 20503.

1. AGENCY USE ONLY (Leave blank)	2. REPORT DATE	3. REPORT TYPE AND DATES COVERED
	13 August 1992	Reprint

4. TITLE AND SUBTITLE

An Experimental Investigation of Thermospheric Structure Near an Auroral Arc

5. FUNDING NUMBERS

PE 62101F
PR 4643
TA 11
WU 06

6. AUTHOR(S)

R.W. Eastes, T.L. Killeen*, Q. Wu*, J.D. Winningham**, W.R. Hoegy#, L.E. Wharton#, G.R. Carignan*

7. PERFORMING ORGANIZATION NAME(S) AND ADDRESS(ES)

Phillips Lab/GPIM
Hanscom AFB
Massachusetts 01731-5000

8. PERFORMING ORGANIZATION REPORT NUMBER

PL-TR-92-2208

DTIC
ELECTE
AUG 26 1992
S D
C

9. SPONSORING/MONITORING AGENCY NAME(S) AND ADDRESS(ES)

10. SPONSORING/MONITORING AGENCY REPORT NUMBER

11. SUPPLEMENTARY NOTES *Space Physics Research Laboratory, Dept of Atmospheric,Oceanic, and Space Sciences, University of Michigan, Ann Arbor **Southwest Research Institute San Antonio, Texas #NASA Goddard Space Flight Center, Greenbelt, Maryland - Reprinted from Journal of Geophysical Research, Vol. 97, No. A7, pages 10,539-10, 549, July 1, 1992

12a. DISTRIBUTION/AVAILABILITY STATEMENT

Approved for public release; Distribution unlimited

12b. DISTRIBUTION CODE

13. ABSTRACT (Maximum 200 words)

Observations of thermospheric parameters, made from the Dynamics Explorer 2 (DE 2) spacecraft during three successive orbital crossings of a quiescent dusk sector auroral arc, have been compared with the predictions of three fine-grid auroral arc models. DE 2 measured the ion and neutral winds, electron and neutral temperatures, neutral composition, and energetic auroral electron spectra (5 eV to 32 keV) at ~320 km altitude. These observations were at high spatial and temporal resolution, suitable for comparisons with the models. The observed zonal and meridional neutral winds near the arc were greater than the model predictions, probably because of the presence of stronger electric fields and higher ion and neutral densities during the observations than were used in the models. The measured vertical winds were also larger than the corresponding model values. The DE 2 composition measurements showed a local increase of the N_2/O ratio in the arc, which is interpreted to be a result of the upward motion of N_2-rich air. A reduction in the measured neutral temperature of ~100 K in the arc, relative to temperatures on either side, was found for all three arc crossings. Of the three theoretical models examined, only one shows any tendency for the neutral thermospheric temperature to drop in the auroral arc, and the decrease calculated is significantly less than the observed temperature change. A simple calculation of the adiabatic cooling effect of the observed upward motion yields a temperature drop of ~160 K, comparable with the observed temperature reduction (~100 K).

14. SUBJECT TERMS

Aurora, Auroral arc, Thermospheric structure

15. NUMBER OF PAGES

11

16. PRICE CODE

17. SECURITY CLASSIFICATION OF REPORT	18. SECURITY CLASSIFICATION OF THIS PAGE	19. SECURITY CLASSIFICATION OF ABSTRACT	20. LIMITATION OF ABSTRACT
Unclassified	Unclassified	Unclassified	SAR

NSN 7540-01-280-5500

Standard Form 298 (Rev. 2-89)

JOURNAL OF GEOPHYSICAL RESEARCH, VOL. 97, NO. A7, PAGES 10,539–10,549, JULY 1, 1992

An Experimental Investigation of Thermospheric Structure Near an Auroral Arc

R. W. EASTES,[1] T. L. KILLEEN,[2] Q. WU,[2] J. D. WINNINGHAM,[3] W. R. HOEGY,[4] L. E. WHARTON,[4] AND G. R. CARIGNAN[2]

Observations of thermospheric parameters, made from the Dynamics Explorer 2 (DE 2) spacecraft during three successive orbital crossings of a quiescent dusk sector auroral arc, have been compared with the predictions of three fine-grid auroral arc models. DE 2 measured the ion and neutral winds, electron and neutral temperatures, neutral composition, and energetic auroral electron spectra (5 eV to 32 keV) at ~320 km altitude. These observations were at high spatial and temporal resolution, suitable for comparisons with the models. The observed zonal and meridional neutral winds near the arc were greater than the model predictions, probably because of the presence of stronger electric fields and higher ion and neutral densities during the observations than were used in the models. The measured vertical winds were also larger than the corresponding model values. The DE 2 composition measurements showed a local increase of the N_2/O ratio in the arc, which is interpreted to be a result of the upward motion of N_2-rich air. A reduction in the measured neutral temperature of ~100 K in the arc, relative to temperatures on either side, was found for all three arc crossings. Of the three theoretical models examined, only one shows any tendency for the neutral thermospheric temperature to drop in the auroral arc, and the decrease calculated is significantly less than the observed temperature change. A simple calculation of the adiabatic cooling effect of the observed upward motion yields a temperature drop of ~160 K, comparable with the observed temperature reduction (~100 K).

1. INTRODUCTION

Large-scale numerical modeling of the response of the neutral thermosphere to high-latitude ion convection [e.g., *Cole*, 1971; *Dickinson et al.*, 1971; *Fedder and Banks*, 1972; *Heaps and Megill*, 1975; *Maeda*, 1976; *Straus and Schulz*, 1976; *Mayr and Harris*, 1978; *Volland*, 1979; *Rees et al.*, 1980, 1984*a*, *b*, 1985*a*, *b*; *Fuller-Rowell and Rees*, 1981; *Mikkelsen et al.*, 1981*a*, *b*; *Dickinson et al.*, 1981; *Roble et al.*, 1982, 1988*a*, *b*; *Larsen and Mikkelsen*, 1983; *Mikkelsen and Larsen*, 1983; *Walterscheid and Boucher*, 1984; *Killeen and Roble*, 1984; *Fuller-Rowell et al.*, 1987; *Roble and Ridley*, 1987] has successfully explained many of the experimental observations of the neutral wind [e.g., *Nagy et al.*, 1974; *Hays et al.*, 1979; *Pereira et al.*, 1980; *Heppner and Miller*, 1982; *Killeen et al.*, 1982, 1984, 1986; *Hays et al.*, 1984; *Sica et al.*, 1986; *Meriwether et al.*, 1988; *Hernandez and Killeen*, 1988; *Killeen and Roble*, 1988]. The primary auroral sources of thermospheric momentum and energy are ion drag and Joule heating, respectively. These are often characterized by great spatial and temporal variability. Because of computer time limitations, the large-scale, three-dimensional, numerical models cannot fully resolve the small-scale structures in ion drag and Joule heating associated with discrete auroral features. Therefore these models cannot hope to predict the local thermospheric response accurately. This limitation has prompted the development of high-resolution (~10 km) two-dimensional models of the thermosphere near auroral arcs.

The first of these models, published by *St. Maurice and Schunk* [1981], solved the magnetohydrodynamic equations to simulate the neutral thermospheric response to narrow ion convection channels and plasma density troughs. More recently, *Fuller-Rowell* [1984, 1985] and *Walterscheid et al.* [1985] have independently developed nonlinear high-resolution dynamical models. These models will be referred to by the labels SS, FR, and WLT, respectively. All three models simulate, in two dimensions, the dynamical response of the thermosphere to narrow auroral arcs. The auroral features were given different latitudinal widths in each case (100 km in the SS model, 60 km in the WLT model, and 100 and 500 km in the FR model).

Unfortunately, there is a lack of published experimental data suitable for comparison with the predictions of these dynamical models. Rocket measurements are not suited to the spatial or long-term temporal coverage needed. Satellites have not typically been instrumented to characterize both the auroral arcs themselves and the thermospheric response to the localized forces associated with those arcs. The Dynamics Explorer (DE 2) satellite provided such a data base, with sufficient spatial and temporal coverage to investigate the local energy and momentum sources as well as the dynamical, compositional, and thermal response of the ambient atmosphere. The primary purpose of this paper is to present a study of the high-spatial-resolution (~8 km) thermospheric wind, temperature, and composition data from DE 2 for a quiet auroral arc crossing. The secondary purpose is a comparison of these experimental results with predictions from the three high-resolution dynamical models.

In the next section we briefly describe the basic assumptions, input parameters, geometric configurations, limitations, and output results of the three theoretical models. The model discussion is followed, in section 3, by presentation of the high-resolution DE 2 data. In section 4 the DE 2 data and

[1]Phillips Laboratory, Hanscom Air Force Base, Massachusetts.
[2]Space Physics Research Laboratory, Department of Atmospheric, Oceanic, and Space Sciences, University of Michigan, Ann Arbor.
[3]Southwest Research Institute, San Antonio, Texas.
[4]NASA Goddard Space Flight Center, Greenbelt, Maryland.

Paper number 92JA00168.
0148-0227/92/92JA-00168$05.00

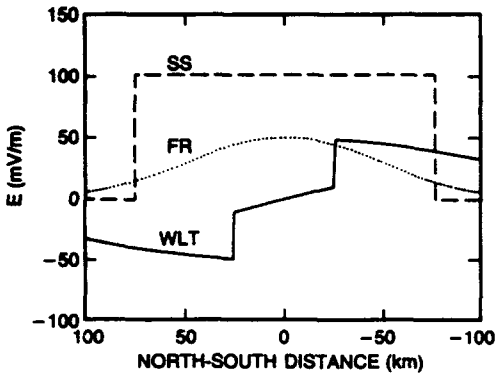

Fig. 1. The latitude profiles of the electric fields used in the models by *St. Maurice and Schunk* [1981] (SS), *Fuller-Rowell* [1984, 1985] (FR), and *Walterscheid et al.* [1985] (WLT). The distances are from the center of the arc.

theoretical model results are critically compared. Finally, in section 5 the results of the study are summarized.

2. Theoretical Models

All three models of the thermosphere near an auroral arc [*St. Maurice and Schunk*, 1981 (SS); *Fuller-Rowell*, 1984, 1985 (FR); *Walterscheid et al.*, 1985 (WLT)] were two dimensional, assuming zonal symmetry along the arc. Each model calculated the dynamical response of the neutral atmosphere to given auroral distributions of electric charge, electric field, and precipitating energetic particles. The models predicted the neutral wind velocities, temperatures, and compositional perturbations, quantities that were measured by instruments on DE 2.

2.1. *Model Descriptions*

The pioneering model of *St. Maurice and Schunk* [1981] solved the zonal and meridional momentum equations, neglecting the nonlinear inertial (or advective) terms. Omitting these terms restricted the applicability of the SS model to subsonic flows. Two other assumptions further limited the range of applicability. First, the SS model did not consider the coupling of the momentum equation with the continuity or energy equation and did not treat vertical motions, restricting the self-consistency of the solution. Second, the SS model was not time dependent and therefore provided only a steady state solution for the dynamical response of the thermosphere to ion drag forcing. St. Maurice and Schunk estimated that the time taken to reach a steady state would typically be a few hours.

For the results shown here, the SS model used an electric field with a latitudinal variation represented by the dashed line labeled SS in Figure 1. Other input parameters used in the model are given in Table 1, with those for the FR and WLT models and the DE 2 observations discussed below. At an altitude of 320 km a charge density of 9×10^4 cm^{-3} was used within 75 km of the center of the arc, dropping by a factor of 10 at greater distances from the arc. The neutral atmosphere used was based on the *Jacchia* [1964] model, with an exospheric temperature (T_∞) of 1400 K.

Unlike the earlier SS model, the WLT and FR models were both nonlinear and time dependent and included the coupling of the momentum, continuity, and energy equations. The time-dependent feature of the WLT and FR models allowed the evolution of the atmospheric response to discrete auroral structures to be followed. Both these models solved the meridional, zonal, and vertical momentum equations. The FR model used pressure coordinates ($z_{max} \approx 350$ km) and also calculated the compositional response of the atmosphere, treating three gas species: O, N_2, and O_2. The WLT model used Cartesian coordinates ($z_{max} = 240$ km) and allowed for variation of composition-dependent quantities.

The electric field used by the FR model is shown in Figure 1 as a dotted line. This line represents the Gaussian latitudinal profile (1° full width at half maximum (FWHM)) assumed for the electric field. The FR model used ion densities from the *Chiu* [1975] model except below 200 km when within the arc, where an enhancement was added. At 320 km the ion density used was $\sim 10^5$ cm^{-3}.

The electric field configuration used by the WLT model is represented by the solid line in Figure 1. The electric field that WLT used, unlike the other models, changed sign at the center of the convection channel. This electric field variation was considered by *Walterscheid et al.* [1985] to be significantly more realistic than that used by Fuller-Rowell. At 240 km (the highest altitude for which the published model results were shown), WLT used an ion density of $\sim 4 \times 10^5$ cm^{-3} within 35 km of the center of the arc, dropping by a factor of 2 at distances further from the arc. Elsewhere, WLT used ion densities from the *Chiu* [1975] model.

TABLE 1. Model Input Parameters

Parameters	SS	FR	WLT	Data
E_{max}, mV/m	100	50	40	50–75
N_{imax}, cm^{-3}	9×10^{4}*	2×10^{5}*	···	6×10^{5}†
	9×10^{4}‡	2×10^{5}‡	4×10^{5}‡	
T_∞, K	1400	700	1000	1200
Elapsed time to equilibrium, hours	NA	3	1	1.5
ΔT_n, K	8*	7‡	≤30‡	−100†
U_{nmax} (zonal, m/s)	200*	300*	···	300–600†
	220‡	240‡	220‡	
V_{nmax} (meridional, m/s)	NA	13‡	16‡	
W_{nmax} (vertical, m/s)	NA	10‡	20‡	<30†
Mean mass (inside arc/outside arc)	···	1.02	···	

Electric fields for the three models are shown in Figure 1. Three center dots mean that the value was not specified by the model. NA is not applicable.

*Values at 320 km altitude.

†Measurements between 310 and 330 km altitude.

‡Values at 240 km altitude.

The SS model used an exospheric temperature of 1400 K (based on the *Jacchia* [1964] model), and the WLT model used the U.S. Standard Atmosphere (1976) model, which has an exospheric temperature of 1000 K. The FR model used a significantly lower exospheric temperature of ~700 K.

2.2. *Model Results*

The results of all three dynamical models were (as expected) dependent upon the input parameters: neutral density, electric fields, and charge distribution as well as (for the two time-dependent models) the elapsed time. Therefore differences in the results are expected to be due to both variation of the input parameters and differences in the model formulations. Any detailed comparison between individual models and experimental data must account for variations in these parameters. However, the gross characteristics of the neutral temperature variations and vertical, zonal, and meridional neutral winds predicted by the models can be compared fruitfully with the DE 2 data. The following is a brief review of the published results from the theoretical models when using the input specifications summarized in Table 1.

The FR and WLT models predicted that the thermospheric temperature near the auroral arc would rise by <30 K at altitudes of 320 km (FR) and 240 km (WLT), respectively. The WLT model predicted a 10- to 28-K overall increase in the neutral temperature at the location of the arc itself relative to temperatures on either side (see Figure 9*a* of *Walterscheid et al.* [1985]). The FR model predicted a ~7-K (or less) temperature increase at 320 km after 3 hours. The auroral heating of the thermosphere predicted by the models could lead to thermospheric composition perturbations. The FR model was the only one of the three to include specific calculations of the composition variations and predicted increases of a factor of ~1.02 in the mean molecular mass at 320 km for the simulated dawn sector auroral arc. No calculations were published for the dusk sector.

Weak vertical and meridional winds were predicted by the theoretical models. The maximum vertical wind values (W_{max}) predicted by the WLT and FR models within the arc were ~10 m/s near altitudes of 240 and 320 km, respectively. As mentioned above, the SS model did not provide calculations of vertical winds. The FR model predicted a maximum meridional wind value (V_{max}) of ~40 m/s at 320 km, while WLT predicted a V_{max} of ~16 m/s at 240 km. The SS model significantly overestimated the meridional wind, presumably because it neglected the pressure gradient forces [*Walterscheid et al.*, 1985].

The strongest winds predicted were in the zonal direction. The SS model predicted maximum zonal winds (U_{max}) of ~200 m/s at 320 km. The FR model predicted a U_{max} of ~300 m/s at 320 km in the dusk sector 3 hours after the initiation of the arc. The FR model also showed a tendency for U_{max} to increase with an increase in the width of the simulated arc. For an arc width of 5° FWHM, the FR model predicted a larger U_{max} (~480 m/s at 300 km after 3 hours). The WLT model predicted a U_{max} of ~220 m/s at 240 km after 1 hour. *Fuller-Rowell* [1985] pointed out that the zonal winds would not necessarily increase with increasing electric fields owing to the counteracting effects of the stronger cross-channel meridional winds.

The SS model used lower ion densities but strong electric fields and higher neutral densities than the other two models. However, all three models predicted zonal winds of the order of a few hundred meters per second near 300 km for elapsed times of the order of hours. The stronger winds predicted by the FR model may be partially a result of lower atmospheric densities near 300 km when T_∞ = 700 K. Weak (~20 m/s) vertical and meridional winds and a temperature increase of the order of 10 K in the neutral atmosphere (relative to the temperatures occurring before the auroral arc) were predicted by both WLT and FR.

3. EXPERIMENTAL DATA

3.1. *Data Selection*

Comparison of the models with the DE 2 observations can be facilitated by using appropriate data selection criteria. Of particular importance is the spatial resolution of the measurements. Ion winds, energetic electron fluxes, electron temperatures, and electron densities, for example, are all known to have significant variations at scale lengths of ~8 km or less. The velocity of the spacecraft is ~8 km/s. Therefore parameters that vary on this scale (~8 km or less) need to be measured with a temporal resolution of 1 s or less. However, lower spatial resolution should be adequate for the neutral winds and temperatures since they have larger characteristic scale lengths.

Long-term temporal resolution is also important. The models treat the development of neutral winds on time scales of hours; therefore repeated observations of an arc, which is spatially stable for hours, are desirable for comparison with the models. Such a quiescent arc would be observable on a series of orbits since the orbital period for DE 2 was ~1.5 hours. Also, a single discrete arc, being the simplest case, is preferable to multiple arcs.

The availability of measurements crucial to comparisons with the models is another factor in data selection. The Langmuir probe instrument (LANG) [*Krehbiel et al.*, 1981] measured the electron temperature and ion density. The electric fields can be determined from the ion winds which were measured by the ion drift meter (IDM) [*Heelis et al.*, 1981] and the retarding potential analyzer (RPA) [*Hanson et al.*, 1981]. The IDM measured the ion winds in the plane perpendicular to the orbital velocity, and the RPA measured the wind perpendicular to this plane. The neutral atmosphere composition spectrometer (NACS) measured the composition of the neutral atmosphere [*Carignan et al.*, 1981]. The low-altitude plasma instrument (LAPI) [*Winningham et al.*, 1981] measured the energetic electron spectrum between 5 eV and 32 keV. Two instruments measured the motion of the atmosphere resulting from the forcing by the ions. The winds and temperature spectrometer (WATS) [*Spencer et al.*, 1981] measured the neutral temperature and the winds in the plane perpendicular to the satellite velocity vector. The Fabry-Perot interferometer (FPI) [*Hays et al.*, 1981] measured the temperature and the neutral winds parallel to the satellite velocity vector.

Data from orbits 1847, 1848, and 1849 were selected on the basis of the above criteria for detailed study. This series of orbits provided near-complete instrumental coverage, at the best available temporal and spatial resolution, of the thermospheric parameters associated with a single quiescent auroral arc observed during December 1981. Experimental

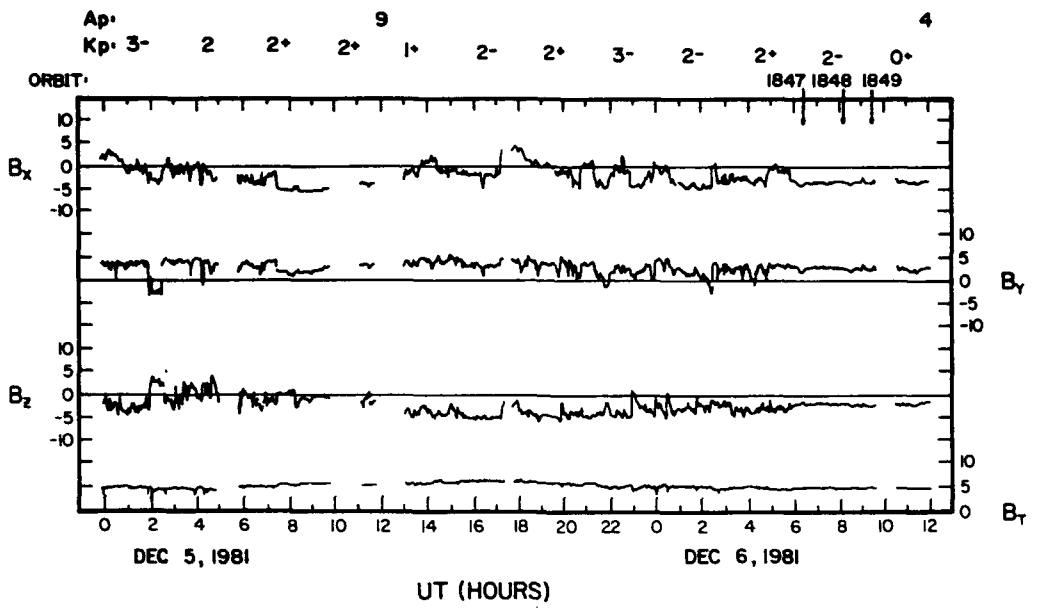

Fig. 2. Geophysical parameters associated with the observations. The arrows beneath the orbit numbers (1847, 1848, and 1849) indicate 1 hour plus the time at which Dynamics Explorer 2 crossed the auroral oval in the dusk sector. One hour was added to compensate for the propagation time of the interplanetary magnetic field since the ISEE satellite, which made the measurements, was between the Sun and the Earth.

data from the LAPI, LANG, IDM, and NACS instruments were available for these orbital passes at 1-s or better resolution. Data from the WATS instrument were available at 2- to 8-s resolution, and data from the FPI instrument were available at ~16 s resolution. During December 1981 the DE 2 orbit was in the dawn-dusk plane, and the spacecraft altitude was ~310 km (close to the altitudes considered in the theoretical models discussed above) when crossing the arc in the dusk auroral zone.

Various geophysical parameters associated with these observations are shown in Figure 2. The *Kp* and *Ap* indices indicate that the geomagnetic conditions were quiet during the observations. The ISEE 3 satellite measurements of the interplanetary magnetic field (IMF) component magnitudes are also shown in Figure 2. The arrows beneath the orbit numbers are calculated from the time of the orbits with a 1-hour universal time (UT) shift incorporated to allow for the propagation time of the IMF from the ISEE 3 location to the auroral ionosphere.

All three orbits crossed almost the same region of the auroral zone. This can be seen in Figure 3, where the tracks of the satellite are plotted in magnetic coordinates. Also shown is a Feldstein statistical auroral oval [*Feldstein*, 1963] which was computed using *Holzworth and Meng*'s [1975] mathematical representation of the oval for $Q = 2$.

3.2. *Discussion of the Data*

Plate 1 illustrates the comprehensive DE 2 data set for orbit 1849. In this plot, time increases from left to right, as the spacecraft traversed the northern hemisphere high-latitude region from dawn to dusk. Plate 1*a* contains the LAPI data from the detector designed to measure precipitating electrons at a pitch angle of 45°. As the satellite crosses the dawn auroral oval (near 0833 UT), numerous discrete auroral arcs (inverted Vs) can be seen in the electron spectra, while in the dusk auroral oval (near 0840 UT) there is only one such arc. Plate 1*b* shows the measured electron temperature (T_e) and ion density (N_i) data from the Langmuir probe. The correlation between the temperature of the thermal electrons and the intensities of the precipitating electrons measured by LAPI is evident.

The zonal component of the ion and neutral winds and the meridional component of the neutral wind are shown in Plate 1*c*. The familiar pattern of the neutral winds for IMF B_y positive [*McCormac et al.*, 1985] is apparent. In this plot, U_i (zonal ion wind) and U_n (zonal neutral wind) positive velocities are sunward, and for V_n (meridional neutral wind), positive velocities are in the direction of the space-

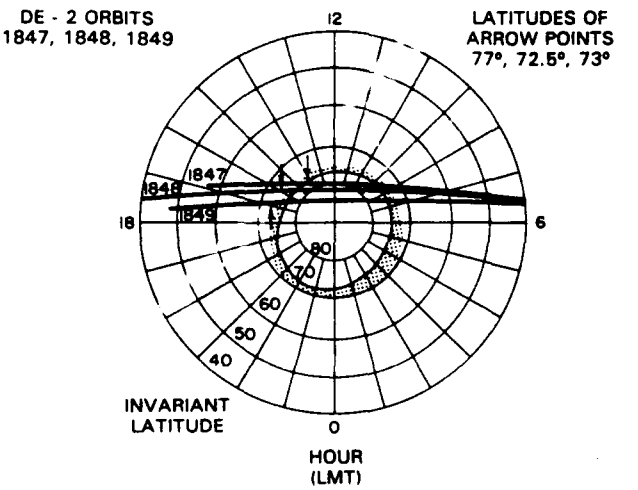

Fig. 3. Orbits 1847, 1848, and 1849 by Dynamics Explorer 2 are shown in magnetic coordinates (invariant latitude and magnetic local time). The shaded area is the Feldstein statistical auroral oval as parameterized by *Holzworth and Meng* [1975].

Plate 1. Data collected by Dynamics Explorer 2 while crossing the northern polar cap during orbit 1849. (*a*) The LAPI data from a pitch angle of 45°. (*b*) Measurements of electron temperature (T_e) and ion density (N_i) by the Langmuir probe. (*c*) The zonal component of the ion (neutral) winds U_i (U_n). Positive zonal winds are sunward. The meridional component of the neutral wind (V_n) is also shown, and V_n positive indicates a poleward wind. (*d*) The vertical components of the ion and neutral winds (W_i and W_n, respectively), and the temperature of the neutral atmosphere (T_n) as measured by the WATS instrument. (*e*) The densities of N_2 and O measured by the NACS instrument. These densities have been normalized to an altitude of 300 km by assuming hydrostatic equilibrium (see text for details).

craft velocity vector: therefore V_n is poleward in both the dawn and dusk sectors. This is at least partially a result of the orientation of the orbit relative to the auroral oval, as shown in Figure 3, and can be seen more clearly in a polar plot of the neutral winds shown in Figure 4. The maximum electric field strength, derived from the IDM measurements, is ~50 m V/m in the dusk sector aurora and ~70 m V/m in the dawn sector aurora.

The vertical components of both the ion (W_i) and neutral (W_n) winds and the neutral temperatures (T_n) measured by WATS (represented by a blue line) are shown in Plate 1*d*. The temperature of the neutral atmosphere increased in the dawn aurora, but such an increase was not seen in the dusk sector.

The heating of the neutral atmosphere is reflected by the increased molecular nitrogen density (relative to the atomic oxygen density) seen in both the dawn and dusk sectors as shown in Plate 1*e*. Heating causes N_2-rich lower-altitude air

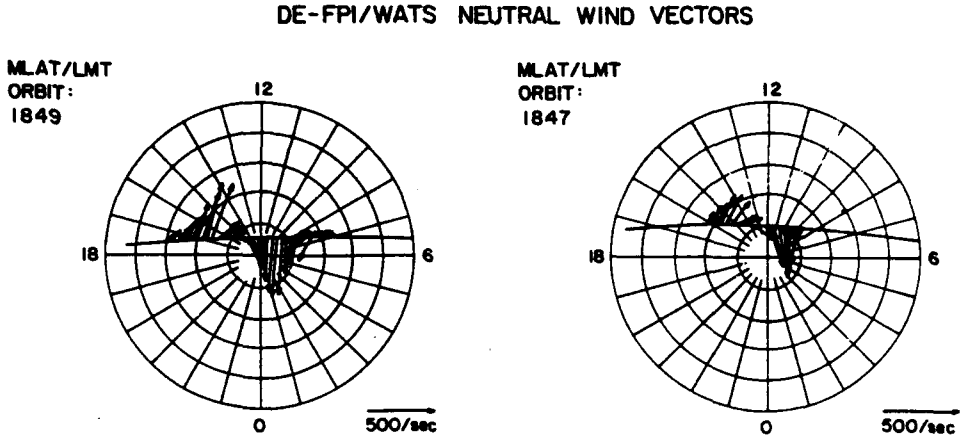

Fig. 4. Polar plots of the neutral winds measured during orbits 1849 and 1847.

to move upward, resulting in an increase in the N_2/O ratio. These data are from the NACS instrument, and they have been normalized to 300 km using a barometric law correction ($e^{-mg/kT}$ where $T = 1200 - [1.5 \times (\text{geographic latitude})]$), in an attempt to remove the altitude dependence of the densities.

Since the dusk sector auroral arc meets the single-arc criterion mentioned above, we will discuss the dusk sector data in more detail. In Figure 5 the data from the quiescent dusk auroral arc crossing during orbit 1849 have been expanded and plotted with respect to invariant latitude to highlight the auroral arc. Figures 6 and 7 show similar data from the two previous orbits (1848 and 1847, respectively). For all three orbits, the position of the single broadest peak in the electron temperature coincided with the peak of the energetic electron energy deposition rate. During orbit 1849 a strong, isolated peak in T_e coincided with elevated intensities of precipitating energetic electrons. The electron temperature enhancements were similar for orbits 1847 and 1848. The hot electrons between 70° and 75° latitude seen in the first two orbits (Figures 6 and 7) had almost disappeared by the time of the arc crossing on orbit 1849 (Figure 5). This change indicates decreased electron heating in that region.

The electron and ion densities were also measured by the Langmuir probe. The electron densities in the region around the discrete auroral arc were similar for all three orbits. Within ±1° from the center of region of highest energy input by electron precipitation, the precipitation was correlated with N_i and T_e.

The neutral wind patterns and velocities, in the zonal direction, were almost identical for the first two orbits. The maximum velocities were between 300 and 400 m/s (Figures 6 and 7). For orbit 1849 (Figure 5) the maximum velocity had increased to almost 600 m/s, and this peak was poleward (in magnetic coordinates) of the peak observed on the previous two orbits. This change in position is attributed to a poleward movement of the zonal component of the ion wind. From orbits 1848 to 1849 the ion wind pattern shifted poleward and decreased in speed.

The meridional component of the neutral wind (V_n) is strong (200 m/s) and poleward in both orbits 1849 and 1847 (meridional wind data for orbit 1848 are not available). Vertical neutral winds (W_n) in the upward direction were seen in all three orbits ($< \sim 30$ m/s).

The most unexpected feature of these data was the neutral atmosphere temperatures. For all three orbits, the lowest temperatures were correlated with the strongest zonal neutral wind measured by WATS. For orbits 1847 and 1849 the lowest observed temperatures were ~100 K lower than those temperatures observed on either side of the auroral arc. While the spacecraft crossed the auroral arc, its altitude was decreasing and had not yet reached a minimum. Thus the observed temperature minima were not caused by the altitude change of the satellite. These temperature minima were localized and were clearly correlated with the location of the discrete auroral arc. Such a temperature minimum was not seen in the dawn oval and has not been previously identified. A summary of the observations during the DE 2 auroral arc crossings is given in Table 1, along with the results from the model calculations.

4. Comparisons Between Experimental Data and Theoretical Models

As noted earlier, the observed temperature of the neutral atmosphere (T_n) is lower in the dusk sector auroral arc than in the adjacent atmosphere. This decrease is seen in all three orbits, and the minimum in T_n is correlated with the maximum in the zonal component of the neutral wind (U_n; see Figures 5, 6, and 7).

Fuller-Rowell [1985] and *Walterscheid et al.* [1985] presented latitudinal profiles of the neutral temperature perturbations in their models. Both predicted higher temperatures in the presence of an auroral arc. The WLT model, however, did predict a local temperature minimum in the center of the arc at 220 km, relative to temperatures outside the arc. But this neutral temperature minimum was only a few degrees lower than the adjacent temperature values (see Figure 9*a* of *Walterscheid et al.* [1985]), and it was not seen after ~10 min. The minima observed at higher altitudes (310–330 km) were an order of magnitude greater than predicted by the model. The observed minima were ~100 K below adjacent values. The WLT model is reported to yield such a minimum at higher altitudes (L. Lyons, personal communication, 1989). According to WLT, this temperature reduction is due to adiabatic cooling of the atmosphere resulting from "overshoot" of parcels that have been accelerated upward by buoyancy forces or by the converging meridional flow. The strongest upward wind in their model was about 15 m/s, at

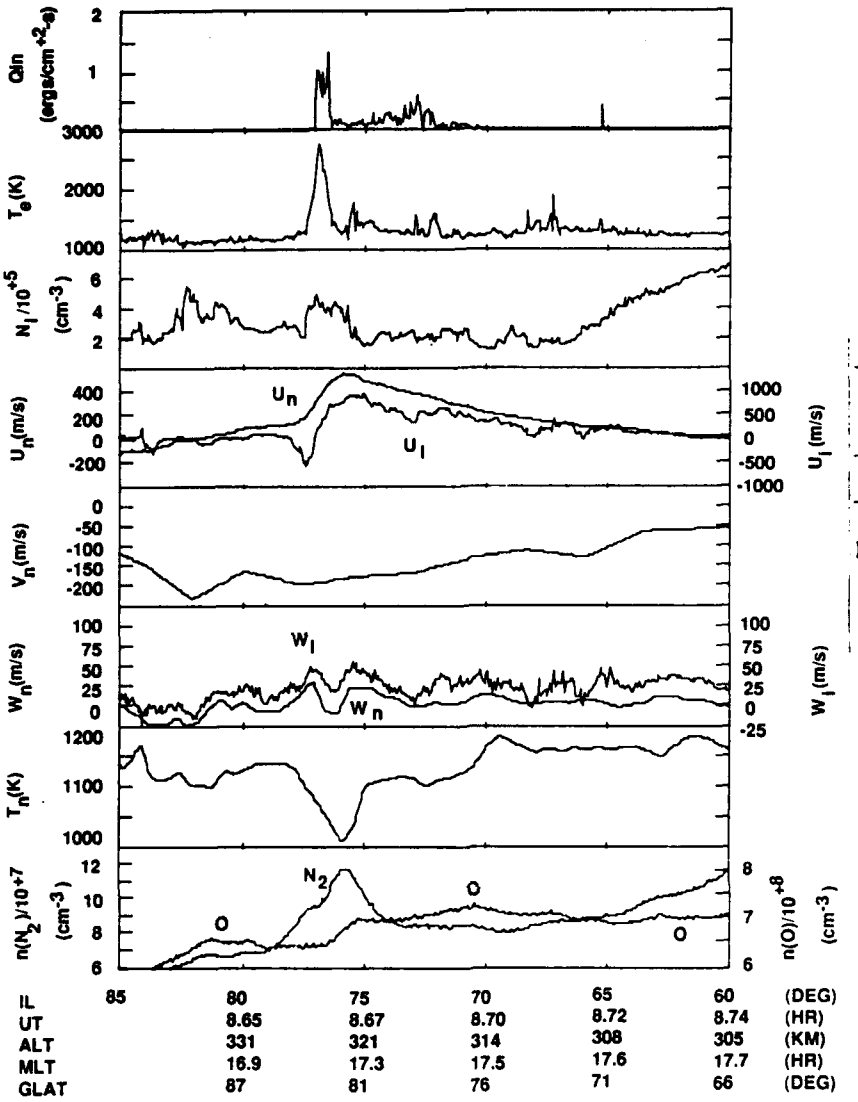

Fig. 5. An expanded plot of the data from the dusk auroral oval during orbit 1849. In the top panel the total energy deposition rate by precipitating electrons is shown. The remaining panels contain the same information as those in Plate 1. T_e is the electron temperature, N_i is the ion density, U_n (U_i) is the zonal component of the neutral (ion) wind, V_n is the meridional component of the neutral wind, W_n (W_i) is the vertical component of the neutral (ion) wind, T_n is the neutral temperature, $n(N_2)$ is the number density of molecular nitrogen, and $n(O)$ is the number density of atomic oxygen. The invariant latitude, universal time, altitude, magnetic local time, and geographic latitude are given at the bottom.

~15 min after the initiation of the simulated auroral arc. While the cooling observed in the WLT model was attributed to waves and the observed cooling seems to persist longer than is appropriate for waves, the idea of adiabatic cooling due to vertical transport may apply.

To determine whether adiabatic cooling can account for such a large reduction in temperature, we performed a simple calculation using a vertical wind of the magnitude observed within the arc. First, we estimated the altitude change for parcels of gas in the region of the arc, using compositional measurements as a reference. The observed N_2/O ratio was higher (0.17) at the location of the auroral arc (see bottom panel in Figure 5). This ratio provided an estimate of the altitude where the individual gas parcels originated. According to the MSIS-86 (mass spectrometer and incoherent scatter 1986) model [*Hedin*, 1987], N_2/O is approximately 0.17 at an altitude of 282 km, where the neutral temperature T_1 is 1027 K and the neutral density ρ_1 is 5.24×10^{-14} g/cm^3. In the region near the arc (bottom panel of Figure 5), N_2/O is ~0.13, approximately the MSIS-86 value at 304 km, where $T_2 = 1032$ K, and $\rho_2 = 3.46 \times 10^{-14}$ g/cm^3. A simple calculation of the adiabatic cooling for parcels of gas moving from an altitude of 282 km to 304 km ($T_1{\rho_1}^{0.4} = T_3{\rho_2}^{0.4}$) gives a final temperature of the parcels, T_3, of 870 K. The temperature drop is $T_2 - T_3 = 162$ K. This temperature difference, based on adiabatic motion of the parcels, is commensurate with that observed by DE 2 (~100 K). Nonadiabatic heating processes, such as particle precipitation, would explain at least part of the difference.

Although the measured zonal velocities were higher than those modeled, this difference is consistent with the stronger electric field and higher ion densities in the observations than were used in the models. Caution is necessary, however,

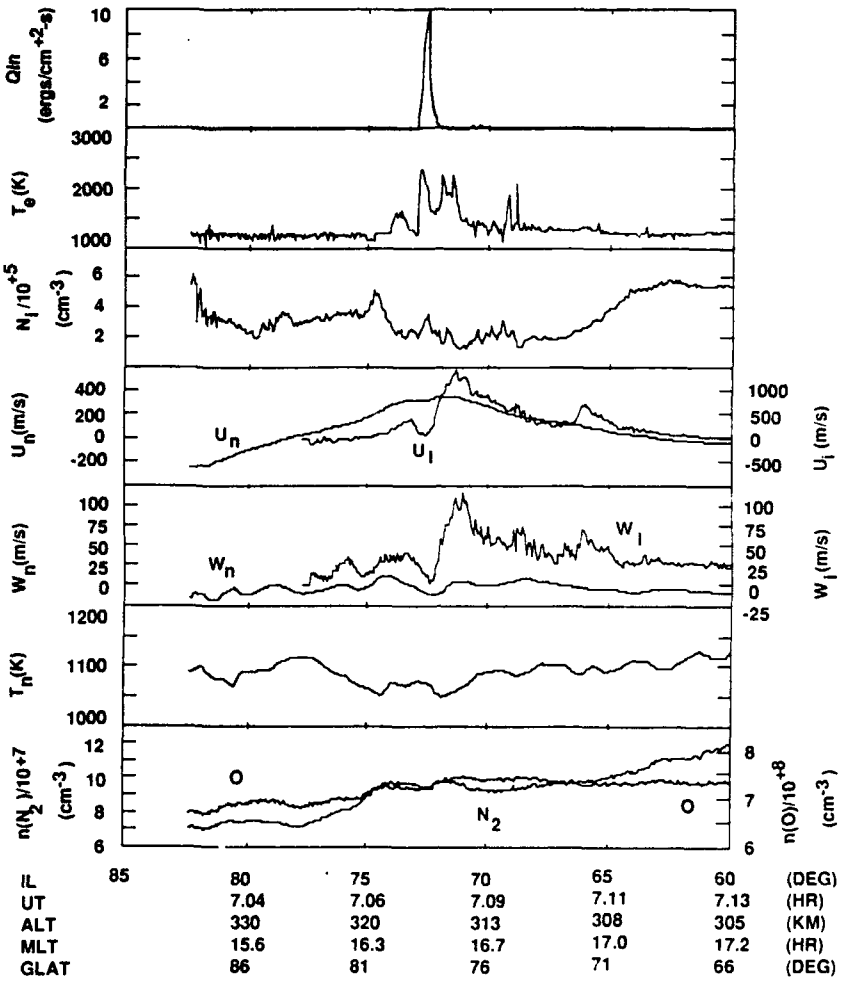

Fig. 6. The same as Figure 5 but for orbit 1848.

since the increased forcing resulting from a stronger electric field will not necessarily lead to higher neutral wind velocities, because of the resulting enhanced crosswinds [*Fuller-Rowell*, 1985]. The electric field in the dusk auroral oval (50–75 mV/m), derived from the measured ion winds, was slightly stronger than that used in the FR and WLT models (see Table 1 and Figure 1).

Larger ion densities may be responsible for the observed zonal winds being stronger than the modeled winds. When the ratio of the ion-neutral collision frequency to the ion gyrofrequency is $<<1$ (approximately true at 310 km), the ion drag force on the neutral atmosphere is simply proportional to the collision frequency of ions and neutrals. This collision frequency is directly proportional to the ion density and is not significantly influenced by the neutral density. Therefore the stronger forcing during orbits 1848 and 1849 might lead to the larger than modeled velocity of the neutral wind (~500 m/s, zonal).

The measured meridional wind velocities were larger on the poleward side of the maximum in U_n than on the equatorward side. All three models predicted much weaker meridional winds (~50 m/s) than were observed. Meridional winds at high latitudes are strongly UT dependent, as a result of the relative orientation of the geomagnetic and geographic poles. Since the neutral winds typically flow parallel to the auroral oval, it can be seen from Figure 3 that a strong velocity component (meridional) parallel to the satellite velocity vector should be observed. The FPI measured meridional winds of ~125 m/s equatorward of the auroral oval (Plate 1 and Figures 5 and 7). The meridional neutral winds at the lower latitudes are attributed to solar heating. This wind allows the development of the strong zonal winds according to *Fuller-Rowell* [1984].

The structure of the electric field on orbit 1849 closely resembled that used by *Walterscheid et al.* [1985], who based their parameters on the observations of *Evans et al.* [1977]. The polarity of the measured electric field changed at the center of the arc, like the electric field used in the model. Similar electric field structures were seen in the dawn oval (Plate 1). The neutral winds observed in the dawn sector, however, will be driven by the time-integrated effect of these multiple convection features, leading to more complex local behavior than is seen for the single quiescent dusk sector arc. A more thorough comparison of the models and data will require detailed matching of input parameters with measured auroral arc features.

5. SUMMARY

A critical comparison between DE 2 satellite measurements of upper thermospheric winds, temperatures, and composition in the vicinity of a single, quiescent auroral arc

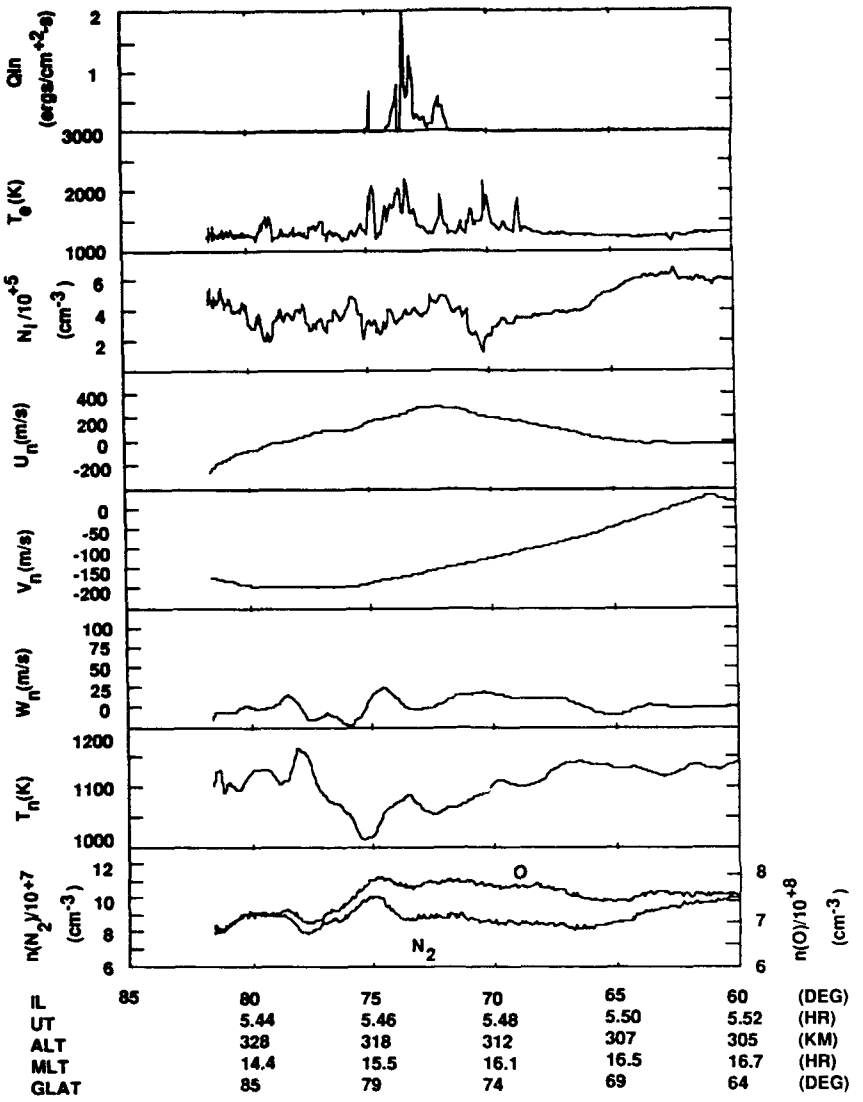

Fig. 7. The same as Figure 5 but for orbit 1847.

with the predictions of three high-resolution models has been performed. The experimental data were carefully selected to provide an optimum comparison with the theoretical predictions of the thermospheric response to localized auroral forcings. The observed zonal neutral winds were larger than those calculated by the models, probably because of the weaker electric fields and lower ion and neutral densities used in the models (see Table 1). The models also predicted much weaker meridional and vertical winds than those observed. An unexpected observation was a localized neutral temperature minimum at the arc ($\Delta T \approx 100$ K). This temperature drop probably results from adiabatic cooling due to pressure changes resulting from vertical displacements of the atmosphere. An increase in the N_2/O ratio near the auroral arc was observed, which is also attributed to the vertical displacements from the N_2-rich lower thermosphere. A rough estimation of the effects of adiabatic cooling based on the observed auroral N_2/O ratio and the MSIS-86 model yielded a temperature drop of ~160 K, commensurate with the observed temperature minimum if nonadiabatic heating is also considered. Stronger upward winds in the models might lead to more prominent adiabatic cooling effects than have been predicted to date. Further theoretical work with more realistic auroral inputs will be needed to resolve the theory-experiment discrepancies.

Acknowledgments. This work was supported by NASA grants NAG5-465 and NAGW-1535 and NSF grant ATM-8918476 to the University of Michigan and by NASA contract NAS5-33031 to the Southwest Research Institute. One of the authors, R. Eastes, thanks Barbara Emery for supplying calculations from her satellite track model.

The Editor thanks S. W. Bougher and J.-P. St. Maurice for their assistance in evaluating this paper.

REFERENCES

Carignan, G. R., B. P. Block, J. C. Maurer, A. E. Hedin, C. A. Reber, and N. W. Spencer, The neutral mass spectrometer on Dynamics Explorer B, *Space Sci. Instrum.*, *5*, 429–441, 1981.

Chiu, Y. T., An improved phenomenological model of global ionospheric density, *J. Atmos. Terr. Phys.*, *37*, 1563–1570, 1975.

Cole, K. D., Electrodynamic heating and movement of the thermosphere, *Planet. Space Sci.*, *19*, 59–75, 1971.

Dickinson, R. E., R. G. Roble, and E. C. Ridley, Response of the neutral thermosphere at *F*-layer heights to interaction of a global

wind with anomalies of ionization, *J. Atmos. Sci.*, *28*, 1280–1293, 1971.

Dickinson, R. E., E. C. Ridley, and R. G. Roble, A three-dimensional general circulation model of the thermosphere, *J. Geophys. Res.*, *86*, 1499–1512, 1981.

Evans, D. S., N. C. Maynard, J. Troim, T. Jacobsen, and A. Egeland, Auroral vector electric field and particle comparisons, 2, Electrodynamics of an arc, *J. Geophys. Res.*, *82*, 2235–2249, 1977.

Fedder, J. A., and P. M. Banks, Convection electric fields and polar thermospheric winds, *J. Geophys. Res.*, *77*, 2328–2340, 1972.

Feldstein, Ya. I., On morphology of auroral and magnetic disturbances at high latitudes, *Geomagn. Aeron.*, *3*, 227, 1963. (*Geomagn. Aeron.*, Engl. Transl., *3*, 183, 1963.)

Fuller-Rowell, T. J., A two-dimensional, high-resolution, nested-grid model of the thermosphere, 1, Neutral response to an electric field "spike," *J. Geophys. Res.*, *89*, 2971–2990, 1984.

Fuller-Rowell, T. J., A two-dimensional, high-resolution, nested-grid model of the thermosphere, 2, Response of the thermosphere to narrow and broad electrodynamic features, *J. Geophys. Res.*, *90*, 6567–6586, 1985.

Fuller-Rowell, T. J., and D. Rees, Global dynamic response of the thermosphere to a geomagnetic substorm, *J. Atmos. Terr. Phys.*, *43*, 701–721, 1981.

Fuller-Rowell, T. J., S. Quegan, D. Rees, R. J. Moffett, and G. J. Bailey, Interactions between neutral thermospheric composition and the polar ionosphere using a coupled ionosphere-thermosphere model, *J. Geophys. Res.*, *92*, 7744–7748, 1987.

Hanson, W. B., R. A. Heelis, R. A. Power, C. R. Lippincott, D. R. Zuccaro, B. J. Holt, L. H. Harmon, and S. Sanatani, The retarding potential analyzer for Dynamics Explorer B, *Space Sci. Instrum.*, *5*, 503–510, 1981.

Hays, P. B., J. W. Meriwether, and R. G. Roble, Nighttime thermospheric winds at high latitudes, *J. Geophys. Res.*, *84*, 1905–1913, 1979.

Hays, P. B., T. L. Killeen, and B. C. Kennedy, The Fabry-Perot interferometer on Dynamics Explorer, *Space Sci. Instrum.*, *5*, 395–416, 1981.

Hays, P. B., et al., Observations of the dynamics of the polar thermosphere, *J. Geophys. Res.*, *89*, 5597–5612, 1984.

Heaps, M. G., and L. R. Megill, Circulation in the high-latitude thermosphere due to electric fields and Joule heating, *J. Geophys. Res.*, *80*, 1829–1831, 1975.

Hedin, A. E., MSIS-86 thermospheric model, *J. Geophys. Res.*, *92*, 4649–4662, 1987.

Heelis, R. A., W. B. Hanson, C. R. Lippincott, D. R. Zuccaro, L. H. Harmon, B. J. Holt, J. E. Doherty, and R. A. Power, The ion drift meter for Dynamics Explorer B, *Space Sci. Instrum.*, *5*, 511–521, 1981.

Heppner, J. R., and M. L. Miller, Thermospheric winds at high latitudes from chemical release observations, *J. Geophys. Res.*, *87*, 1633–1647, 1982.

Hernandez, G., and T. L. Killeen, Optical measurements of winds and temperatures in the upper atmosphere, in COSPAR International Reference Atmosphere: 1986, I. Thermosphere models, *Adv. Space Res.*, *8*(5–6), 149–214, 1988.

Holzworth, R. H., and C.-I. Meng, Mathematical representation of the auroral oval, *Geophys. Res. Lett.*, *2*, 377–380, 1975.

Jacchia, L. G., Static diffusion models of the upper atmosphere with empirical temperature profiles, *Smithson. Contrib. Astrophys.*, *8*, 215–257, 1964.

Killeen, T. L., and R. G. Roble, An analysis of the high-latitude thermospheric wind pattern calculated by a thermospheric general circulation model, 1, Momentum forcing, *J. Geophys. Res.*, *89*, 7509–7522, 1984.

Killeen, T. L., and R. G. Roble, Thermosphere dynamics: Contributions from the first five years of the Dynamics Explorer Program, *Rev. Geophys.*, *26*, 329–367, 1988.

Killeen, T. L., P. B. Hays, N. W. Spencer, and L. E. Wharton, Neutral winds in the polar thermosphere as measured from Dynamics Explorer, *Geophys. Res. Lett.*, *9*, 957–960, 1982.

Killeen, T. L., P. B. Hays, G. R. Carignan, R. A. Heelis, W. B. Hanson, N. W. Spencer, and L. H. Brace, Ion-neutral coupling in the high-latitude *F* region: Evolution of ion heating terms from Dynamics Explorer B, *J. Geophys. Res.*, *89*, 7495–7508, 1984.

Killeen, T. L., et al., Mean neutral circulation in the winter polar *F* region, *J. Geophys. Res.*, *91*, 1633–1649, 1986.

Krehbiel, J. R., L. H. Brace, R. F. Theis, W. H. Pinkus, and R. B. Kaplan, The Dynamics Explorer Langmuir probe instrument, *Space Sci. Instrum.*, *5*, 493–502, 1981.

Larsen, M. F., and I. S. Mikkelsen, The dynamic response of the high-latitude thermosphere and geostrophic adjustment, *J. Geophys. Res.*, *88*, 3158–3168, 1983.

Maeda, H., Neutral winds and ion drift in the polar ionosphere caused by convection electric fields, *J. Atmos. Terr. Phys.*, *38*, 197–205, 1976.

Mayr, H. G., and I. Harris, Some characteristics of electric field momentum coupling with the neutral atmosphere, *J. Geophys. Res.*, *83*, 3327–3336, 1978.

McCormac, F. G., T. L. Killeen, E. Gombosi, P. B. Hays, and N. W. Spencer, Configuration of the high-latitude thermosphere neutral circulation for IMF B_y negative and positive, *Geophys. Res. Lett.*, *12*, 155–158, 1985.

Meriwether, J. W., T. L. Killeen, F. G. McCormac, A. G. Burns, and R. G. Roble, Thermosphere winds in the geomagnetic polar cap for solar minimum conditions, *J. Geophys. Res.*, *93*, 7478–7492, 1988.

Mikkelsen, I. S., and M. F. Larsen, An analytic solution for the response of the neutral atmosphere to the high-latitude convection pattern, *J. Geophys. Res.*, *88*, 8073–8080, 1983.

Mikkelsen, I. S., T. S. Jorgensen, M. C. Kelley, M. F. Larsen, E. Pereira, and J. Vickrey, Neutral winds and electric fields in the dusk auroral oval, 1, Measurements, *J. Geophys. Res.*, *86*, 1513–1524, 1981*a*.

Mikkelsen, I. S., T. S. Jorgensen, M. C. Kelley, M. F. Larsen, and E. Pereira, Neutral winds and electric fields in the dusk auroral oval, 2, Theory and model, *J. Geophys. Res.*, *86*, 1525–1536, 1981*b*.

Nagy, A. F., R. J. Cicerone, P. B. Hays, K. D. McWatters, J. W. Meriwether, W. E. Belon, and C. L. Rino, Simultaneous measurement of ion and neutral motions by radar and optical techniques, *Radio Sci.*, *9*, 315–321, 1974.

Pereira, E., M. C. Kelley, D. Rees, I. S. Mikkelsen, T. S. Jorgensen, and T. J. Fuller-Rowell, Observations of neutral wind profiles between 115 and 175 km altitude in the dayside auroral oval, *J. Geophys. Res.*, *85*, 2935–2940, 1980.

Rees, D., T. J. Fuller-Rowell, and R. W. Smith, Measurements of high latitude thermospheric winds by rocket and ground-based techniques and their interpretation using a three-dimensional, time-dependent, dynamical model, *Planet. Space Sci.*, *28*, 919–932, 1980.

Rees, D., R. W. Smith, P. J. Charleton, F. G. McCormac, N. Lloyd, and A. Steen, The generation of vertical thermospheric winds and gravity waves at auroral latitudes, I, Observations of vertical winds, *Planet. Space Sci.*, *32*, 667–684, 1984*a*.

Rees, D., M. F. Smith, and R. Gordon, The generation of vertical thermospheric winds and gravity waves at auroral latitudes, II, Theory and numerical modeling of vertical winds, *Planet. Space Sci.*, *32*, 685–705, 1984*b*.

Rees, D., et al., The westward thermospheric jet-stream of the evening auroral oval, *Planet. Space Sci.*, *33*, 425–456, 1985*a*.

Rees, D., R. Gordon, T. J. Fuller-Rowell, M. Smith, G. R. Carignan, T. L. Killeen, P. B. Hays, and N. W. Spencer, The composition, structure, temperature, and dynamics of the upper thermosphere in the polar regions during October to December, 1981, *Planet. Space Sci.*, *33*, 617–666, 1985*b*.

Roble, R. G., and E. C. Ridley, An auroral model of the NCAR thermospheric general circulation model (TGCM), *Ann. Geophys., Ser. A*, *5*(6), 369–382, 1987.

Roble, R. G., R. E. Dickinson, and E. C. Ridley, Global circulation and temperature structure of thermosphere with high-latitude plasma convection, *J. Geophys. Res.*, *87*, 1599–1614, 1982.

Roble, R. G., T. L. Killeen, N. W. Spencer, R. A. Heelis, P. H. Reiff, and J. D. Winningham, Thermospheric dynamics during November 21–22, 1981: Dynamics Explorer measurements and thermospheric general circulation model predictions, *J. Geophys. Res.*, *93*, 209–225, 1988*a*.

Roble, R. G., E. C. Ridley, A. D. Richmond, and R. E. Dickinson, A coupled thermosphere/ionosphere general circulation model, *Geophys. Res. Lett.*, *15*, 1325–1328, 1988*b*.

Sica, R. J., M. H. Rees, G. J. Romick, G. Hernandez, and R. G.

Roble, Auroral zone thermosphere dynamics, 1, Averages, *J. Geophys. Res.*, *91*, 3231–3244, 1986.

Spencer, N. W., L. E. Wharton, H. B. Niemann, A. E. Hedin, G. R. Carignan, and J. C. Maurer, The Dynamics Explorer wind and temperature spectrometer, *Space Sci. Instrum.*, *5*, 417–428, 1981.

St. Maurice, J.-P., and R. W. Schunk, Ion-neutral momentum coupling near discrete high-latitude ionospheric features, *J. Geophys. Res.*, *86*, 11,299–11,321, 1981.

Straus, J. M., and M. Schulz, Magnetospheric convection and upper atmospheric dynamics, *J. Geophys. Res.*, *81*, 5822–5832, 1976.

Volland, H., Magnetospheric electric fields and currents and their influence on large scale thermospheric circulation and composition, *J. Atmos. Terr. Phys.*, *41*, 853–866, 1979.

Walterscheid, R. L., and D. J. Boucher, Jr., A simple model of the transient response of the thermosphere to momentum forcing, *J. Atmos. Sci.*, *41*, 1062–1072, 1984.

Walterscheid, R. L., L. R. Lyons, and K. E. Taylor, The perturbed neutral circulation in the vicinity of a symmetric stable auroral arc, *J. Geophys. Res.*, *90*, 12,235–12,248, 1985.

Winningham, J. D., J. L. Burch, N. Eaker, V. A. Blevins, and R. A. Hoffman, The low latitude plasma instrument (LAPI), *Space Sci. Instrum.*, *5*, 465–475, 1981.

G. R. Carignan, T. L. Killeen, and Q. Wu, Space Physics Research Laboratory, University of Michigan, 2455 Hayward, Ann Arbor, MI 48109.

R. W. Eastes, Phillips Laboratory/GPIM, Hanscom Air Force Base, MA 01731-5000.

W R. Hoegy and L. E. Wharton, NASA Goddard Space Flight Center, Code 614, Greenbelt, MD 20771.

J. D. Winningham, Southwest Research Institute, P. O. Drawer 28510, San Antonio, TX 78228-0510.

(Received January 28, 1991;
revised December 2, 1991;
accepted January 16, 1992.)